

Design of a Magnetic-Geared Outer-Rotor Permanent-Magnet Brushless Motor for Electric Vehicles

K. T. Chau¹, Dong Zhang², J. Z. Jiang², Chunhua Liu¹, and Yuejin Zhang²

¹Department of Electrical and Electronic Engineering, University of Hong Kong, Hong Kong, China

²Department of Automation, Shanghai University, Shanghai 200072, China

This paper proposes a novel in-wheel motor, which artfully integrates a magnetic gear into a permanent-magnet brushless (PMBL) DC motor so that they can share a common PM rotor, hence offering both high efficiency and high power density. Moreover, the low-speed requirement for direct driving and the high-speed requirement for compact motor design can be achieved simultaneously. A 2-kW 600/4400-rpm magnetic-geared outer-rotor PMBL DC motor is designed and analyzed, which is particularly suitable for battery-powered electric motorcycles.

Index Terms—Electric vehicle, magnetic gear, outer rotor, permanent-magnet motor.

I. INTRODUCTION

IN-WHEEL permanent-magnet brushless (PMBL) motors are very attractive for electric vehicles, since they can provide electronic differential action [1]. As the wheel speed is only about 600 rpm, the in-wheel PMBL motor is either a low-speed gearless outer-rotor one or a high-speed planetary-geared inner-rotor one. Although the former one takes the advantage of gearless operation, its low-speed operation causes bulky size and heavy weight. On the other hand, although the latter one takes the merits of reduced overall size and weight, the planetary gear inevitably involves transmission loss, acoustic noise, and regular lubrication [2].

Magnetic gearing is becoming attractive, since it offers the advantages of high efficiency, reduced acoustic noise, and maintenance free [3]. The purpose of this paper is to artfully integrate the magnetic gear into a PMBL DC motor so that the low-speed requirement for direct driving and the high-speed requirement for motor design can be achieved simultaneously. A prototype will be designed for an electric motorcycle.

II. DESIGN

Fig. 1 gives a schematic comparison of the proposed magnetic-geared outer-rotor topology and the existing planetary-geared inner-rotor topology for in-wheel motors, in which the tire rim is directly mounted onto the outer rotor of the magnetic gear and the ring gear of the planetary gear, respectively. It can be seen that the proposed topology not only offers reduced size and weight, but also eliminates all the drawbacks due to the mechanical gear.

The detailed configuration of the proposed motor is shown in Fig. 2. The artfulness is the share of a common PM rotor, namely the outer rotor of a PMBL DC motor and the inner rotor of a concentrically arranged magnetic gear. This magnetic gear was first proposed in [3]. The common PM rotor is designed with 3 pole-pairs for high-speed operation, whereas the gear outer rotor is designed with 22 pole-pairs for low-speed operation. The stationary ring sandwiched between the two PM rotors incorporates with steel pole-pieces, which functions to modulate the airgap flux density space harmonics. The stator of the

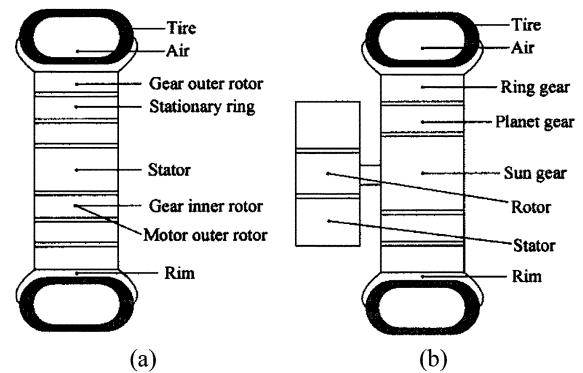


Fig. 1. Cross-sectional views of in-wheel motors. (a) Proposed magnetic-geared topology. (b) Existing planetary-geared topology.

motor adopts a 3-phase winding with fractional slots per pole per phase, hence offering low cogging torque which is highly desirable for vehicle operation.

The principle of operation is similar to a high-speed planetary-geared inner-rotor motor, but with the difference that the proposed motor is an outer-rotor one. Firstly, the stator is fed by 3-phase voltages, which are rated at 220 Hz, to achieve the rated speed of 4400 rpm. Then, the magnetic gear steps down the rated speed to 600 rpm, which in turn boosts up the torque for direct driving.

The torque transmission is based on the modulation of the airgap flux density distributions along the radial and circumferential directions. According to [4], it can be deduced that the number of pole-pairs and the speed of the flux density space harmonics are respectively given by

$$p_{n,k} = |np + ks|, \quad \omega_{n,k} = \frac{np}{|np + ks|} \omega_r \quad (1)$$

where $n = 1, 3, 5, \dots, \infty$, $k = 0, \pm 1, \pm 2, \dots, \pm \infty$, ω_r is the speed of the gear inner rotor, p is the number of pole-pairs of the gear inner rotor, and s is the number of stationary steel pole-pieces. Thus, in order to transmit torque from the gear inner rotor to the gear outer rotor, the number of pole-pairs and the speed of the gear outer rotor must equal $p_{n,k}$ and $\omega_{n,k}$, respectively. Since the combination of $n = 1$ and $k = -1$ results in the highest asynchronous space harmonic, the gear ratio of inner rotor to outer rotor can be obtained as $G_r = |p - s|/p$. Hence, with $p = 3$ and $s = 25$, it yields $G_r = 22/3 = 7.33 : 1$.

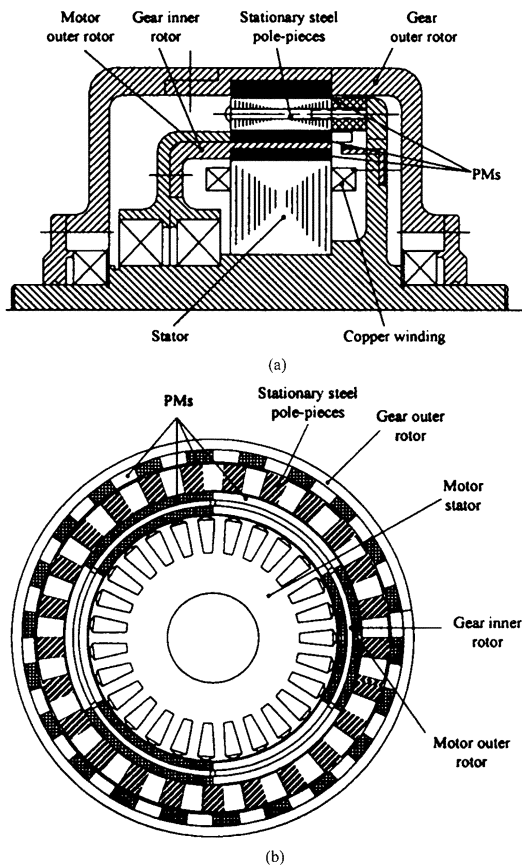


Fig. 2. Proposed motor configuration. (a) Front view. (b) Side view.

TABLE I
DESIGN DATA

Number of phases	3
Rated power	2 kW
Rated phase voltage	36 V
Rated frequency	220 Hz
Rated gear inner-rotor speed	4400 rpm
Rated gear outer-rotor speed	600 rpm
Number of stator slots	27
Number of gear inner-rotor pole-pairs	3
Number of gear outer-rotor pole-pairs	22
Number of stationary steel pole-pieces	25
Number of turns per armature coil	27
Stator diameter	120 mm
Gear inner-rotor outside diameter	142.8 mm
Gear outer-rotor outside diameter	194 mm
Inner airgap length	0.6 mm
Middle airgap length	0.6 mm
Outer airgap length	1 mm
Stack length	40 mm
PM material	38SH NdFeB

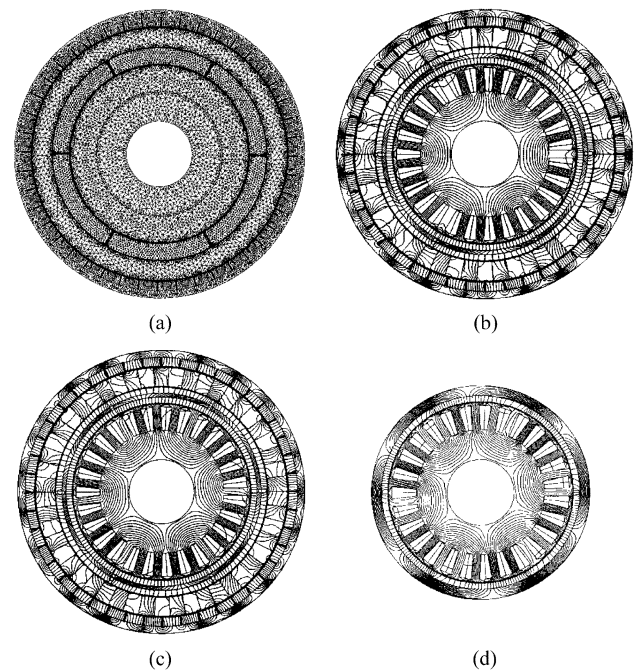


Fig. 3. FEM analysis. (a) Mesh. (b) No-load field distribution. (c) Full-load field distribution. (d) Full-load field distribution with no magnetic gear.

III. RESULTS

Since the proposed motor is composed of two magnetic devices (PMBL DC motor and magnetic gear) and three airgaps (inner, middle, and outer), the finite element method (FEM) is employed. The design data is listed in Table I, which is dedicated to an electric motorcycle. Notice that the outer airgap is relatively wide (1 mm) since the outer rotor needs more mechanical tolerance. Fig. 3(b) and (c) compare the field distributions at no load and full load, whereas Fig. 3(c) and (d) compare the field distributions at full load with and without the magnetic gear. The results show that the armature current field does not cause significant flux distortion on the magnetic gear, whereas the existence of magnetic gear does not significantly affect the PMBL DC motor operation. Fig. 4 shows the back EMF waveforms of the proposed motor at the rated speed, which well agrees with the design data. Then, the radial flux densities in the inner, middle, and outer airgaps are shown in Figs. 5, 6 and 7, respectively. It can be seen that the largest space harmonic is successfully modulated by the stationary steel pole-pieces from 3 pole-pairs in the inner airgap to 22 pole-pairs in the outer airgap.

Since the proposed motor adopts the fractional-slot winding, the cogging torque is confirmed to be very small as shown in Fig. 8. When any two phases of the motor are fed by 100 A, the torque-angle relationship is shown in Fig. 9. Taking into account 3-phase operation, the generated torque in the inner rotor is shown in Fig. 10. It can be found that the maximum value is about 15 Nm which is insufficient to launch the motorcycle.

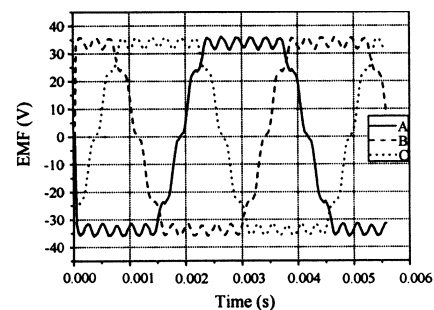


Fig. 4. Back EMF waveforms.

Meanwhile, with the use of magnetic gearing, this torque value can be significantly amplified to about 103 Nm as shown in

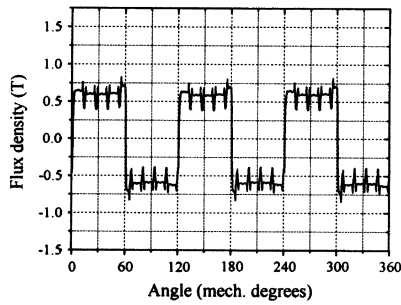


Fig. 5. Radial flux density in inner airgap.

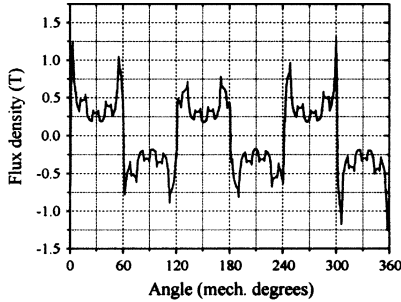


Fig. 6. Radial flux density in middle airgap.

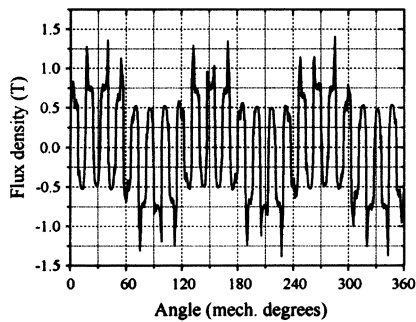


Fig. 7. Radial flux density in outer airgap.

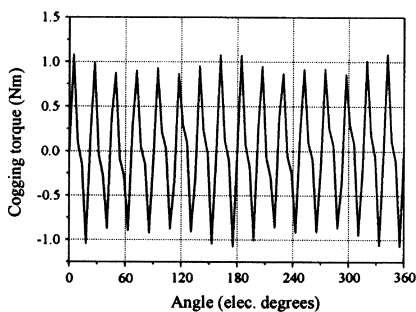


Fig. 8. Cogging torque in inner rotor.

Fig. 11, which is well sufficient to directly launch the motorcycle. In case the load torque is higher than the peak torque transmission capability, the magnetic gear will only slip, rather than suffering from mechanical breakage.

IV. CONCLUSION

A novel magnetic-gearing outer-rotor PMBL DC in-wheel motor has been successfully designed and analyzed. The proposed design can effectively reduce the speed or amplify the

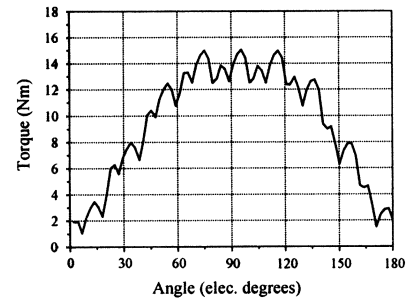


Fig. 9. Torque-angle relationship.

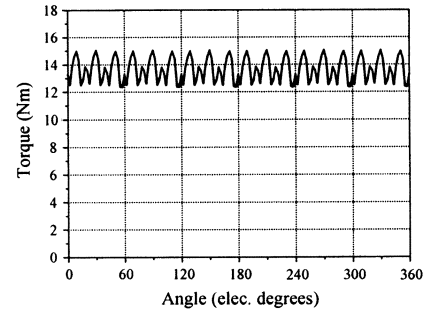


Fig. 10. Generated torque in inner rotor.

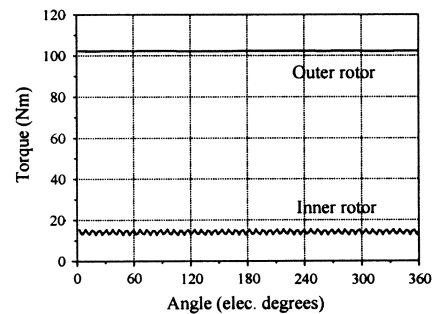


Fig. 11. Comparison of torques in inner and outer rotors.

torque by about 7 times. This in-wheel motor can readily be extended to different sizes of electric vehicles.

ACKNOWLEDGMENT

This work was supported and funded by a grant (Project No. HKU7114/06E) from the Research Grants Council, Hong Kong Special Administrative Region, China.

REFERENCES

- [1] C. C. Chan and K. T. Chau, *Modern Electric Vehicle Technology*. Oxford, U.K.: Oxford Univ. Press, 2001.
- [2] Y. Wang, K. T. Chau, C. C. Chan, and J. Z. Jiang, "Transient analysis of a new outer-rotor permanent-magnet brushless dc drive using circuit-field-torque time-stepping finite element method," *IEEE Trans. Magn.*, vol. 38, no. 2, pp. 1297–1300, Mar. 2002.
- [3] K. Atallah and D. Howe, "A novel high performance magnetic gear," *IEEE Trans. Magn.*, vol. 37, no. 4, pp. 2844–2846, Jul. 2001.
- [4] K. Atallah, S. D. Calverley, and D. Howe, "Design, analysis and realization of a high-performance magnetic gear," *IEE Proc.—Elect. Power Appl.*, vol. 151, no. 2, pp. 135–143, 2004.